Intel Serv Robotics (2011) 4:203–218
DOI 10.1007/s11370-011-0094-7

ORIGINAL RESEARCH PAPER

# Constrained Analytical Trajectory Filter for stabilizing humanoid robot motions

**Karl Muecke · Dennis Hong**

Received: 28 May 2011 / Accepted: 17 June 2011 / Published online: 7 July 2011


**Abstract** Mimicking human motion with a humanoid robot is essential for allowing humanoid robots to be used in service applications. Simply creating motions without considerations for balance and stability or directly copying motion from a human using motion capture and implementing it on a humanoid robot may not be successful because of the difference in physical properties between the human and the humanoid robot, which may cause instability and make it fall. Using the Zero Moment Point as the stability criteria, this work proposes a Constrained Analytical Trajectory Filter as part of an Analytical Motion Filter, which stabilizes a reference motion that can come from human motion capture data, kinematic synthesis, or animation software. The resulting solutions used in the Constrained Analytical Trajectory Filter provide insight into the complex interactions of motion and stability. The solutions were verified in simulation and with hardware, showing that the analytical filter can be successfully applied for stabilizing reference motions for humanoid robots which may be unstable otherwise.

K. Muecke
Virginia Tech, Blacksburg, VA 24061, USA

D. Hong
Department of Mechanical Engineering 0238,
Virginia Tech, Blacksburg, VA 24061, USA
e-mail: dhong@vt.edu

*Present Address:*
K. Muecke (✉)
11500 N. Mopac Expwy,
Austin, TX 78759, USA
e-mail: kmuecke@gmail.com

**Keywords** Humanoid robot · Zero Moment Point · Biped · Motion Filter

## 1 Introduction

### 1.1 Justification

One of the essential aspects in humanoid robotics and walking is the creation of the walking gait. There are a few different schools of thought when it comes to creating walking gaits for humanoid robots. Many researchers take the approach of creating trajectories for the robot's joints to follow. These trajectories are usually based on optimized parametric equations, stability equations, or numerically optimized trajectories through space. In all cases except for gaits created from stability equations, it is difficult to intuitively see *why* the resulting stable walking gaits are stable. Much is hidden by a layer of numeric abstraction. Gaits based on stability equations are very straightforward in conveying *why* the resulting gait is stable and how it was achieved. Unfortunately, these gaits do not leave much leeway for variations in the walking pattern.

Two questions arise when considering the current state of gait generation: Is there a method to stabilize an arbitrary gait that does not rely on numeric optimization schemes? The follow-up question is: Are there closed-form solutions that can stabilize and arbitrary gait, and do these solutions provide some more meaning and insight into gait stability for humanoid robots?

This paper will present a set of analytical solutions that can modify and stabilize an otherwise unstable motion as part of an Analytical Motion Filter (AMF). Additionally, this work discusses experiments in simulation and with hardware to

verify the solutions' validity and provide further insight into the relationship between stability and motion.

## 1.2 Related work

There are at least three primary areas of study in humanoid robot motion: gait generation, motion control, and motion filtering. Gait generation is primarily concerned with coming up with the trajectories needed to create a dynamically stable motion or deriving the necessary dynamic properties of the robot needed to create a stable gait. Motion control is primarily concerned with handling disturbances encountered during the robot's motion. Motion filtering, like gait generation, creates trajectories needed for a dynamically stable motion, but requires an input or reference gait.

### *1.2.1 Gait generation methods*

There are many different kinds of gait generation methods in the field of humanoid robotics. Most of the methods eventually involve some kind of numeric optimization to create a stable gait. However, some methods involve using more interesting approaches that do not require trial and error to generate a stable walking motion.

*Parametric gait synthesis* One of the most common gait generation methods in humanoid robotics, parametric gait generation, is one of the easiest generation methods to implement, but is generally not computationally efficient. Generally, a set of arbitrary parameterized functions describe the motion of the robot. The functions usually describe the ankle, hip, or torso trajectory and orientation. Typically, the functions consists of sines, cosines, and combinations of linear functions [1–8]. In order to create a stable gait, the function parameters are varied in an numeric optimization algorithm whose cost function usually includes: stability, speed, and/or joint torques. There is no consensus on what the "best" or most "optimum" cost function is that is needed to create a gait [9–12]. However, there is a general consensus that the Zero Moment Point (ZMP) criterion is the best for determining the robot's stability.

*Human motion capture* Another popular method for generating gaits is using human motion capture data (HMCD) [13]. Similar to Sect. 1.2.3 and filtering, Dasgupta developed a method to stabilize a reference motion, but focuses on reference motions from HMCD. Again, a numeric optimization function is used to modify the HMCD to follow a desired stable ZMP trajectory.

*Stability-based* An alternative to using optimization functions to tweak gait parameters in order to achieve a stable walking gait is to use dynamic stability equations or stable physical models to generate a gait. This includes: the inverted pendulum model, table-cart model, ZMP-based trajectories, and passive dynamics. The inverted pendulum model is one of the most common simplifications used for generating a walking gait for a humanoid robot [14–19]. By ignoring moments of inertia and the coriolis effects, the robot can be approximated as a collection of point masses. By further assuming that the majority of the mass is located in the upper body of the robot or at least follows the same trajectory as the upper body, then the robot can be simplified to an inverted pendulum, which yields straightforward equations of motion. A slight variation on the inverted pendulum, the table-cart model depicts the robot as a cart able to roll on a table affixed to an inverted pendulum [20]. This accomplishes the same result as allowing the inverted pendulum to change in length.

Takanishi showed in [21] that using a Fast Fourier Transformation (FFT), a gait motion could be derived from a stable ZMP trajectory. Since a walking gait is inherently cyclic, it makes sense that an FFT is an appropriate tool for deriving a solution. Lim showed in [22–24] that hyperbolic sines and cosines could be used as a solution for formulating gaits with a desired ZMP trajectory. Hyperbolic sines and cosines are simply combinations of exponential functions, which reflect the dynamics of an inverted pendulum.

A more popular method for generating bipedal gaits in America is utilizing passive dynamics. Instead of designing a stable gait for a given robot, a robot is designed to naturally perform a stable dynamic gait. McGeer's [25,26] passive dynamic biped walker is one of the most well-known passive dynamic bipeds.

### *1.2.2 Control methods*

In addition to gait generation, stability control is oftentimes needed to create a successfully stable walking robot. Frequently, stability control is closely linked with the gait generation method used. However, since the two can be implemented independently, it is worthwhile to examine control methods separately. Many robots, without an additional layer of stability control, will fall over while performing an initially planned stable walking pattern. The fall occurs because of external disturbances and their perturbation throughout the system. Most advanced humanoid walking robots use a combination of control algorithms to achieve stable humanoid walking in the presence of disturbances [27–33]. Typically, the robots use a force/torque and/or pressure sensor in the feet to measure external loads directly and then accelerometers and rate gyros to determine the robot's orientation.

### *1.2.3 Filtering methods*

Filtering methods differ from generation and control methods in that they generally rely on a previously generated gaits as an input and the control is not used online, but rather in the process of filtering the motion. Filtering motions is not a completely novel concept. Animators and motion researchers commonly modify and filter gaits so that the final subject can successfully perform a version of the original gait [34,35]. For a time, the dynamic stability of the motion was ignored by animators because physically accurate models were not as important. However, recently in an effort to create more realistic animations, physically accurate models and simulations have become more desirable and spurred on more research in the area. Gait researchers are also interested in the idea of filtering motions and have always been concerned with the dynamics and physical meaning behind the gaits. However, most, if not all, methods for filtering gaits are based on numeric algorithms or filters, which can conceal some of the other insight behind why the filtering works.

Witkin [36] describes an animation tool that forms motions for a physically valid human model that obeys constraints and optimization criteria. The method "entails the numerical solution of large constrained optimization problems, for which a variety of standard algorithms exist. These algorithms, while relatively expensive …". In previous efforts, the character animation was created by solving for the character's motion and time-varying muscle forces progressing sequentially through time. Instead, by solving for the muscle forces over the entire time interval, he formulated a model called *spacetime constraints*.

Witkin's key contribution was to allow the effects of constraints to propagate forwards and backwards in time, unlike some previously developed algorithms that only considered the effects of a constraint at a given moment. The animation model character, called "Luxo," was able to perform a variety of physically valid motions specified by the animator. However, for all of the motion generated, numeric solutions were used with optimization functions in order to generate the final motion. Though Witkin helped contribute to creating a more efficient and useful tool for animators, the process does not provide much insight into the stability of the motion.

Tak [37] describes "a constraint-based motion editing technique that on the basis of animator-specified kinematic and dynamic constraints converts a given captured or animated motion to a physically plausible motion". The method is used by viewing the motion as sequential frames. The filter is "basically a concatenation of unscented Kalman filters[s] and … least-squares filter[s]…we can add or remove some or all of the kinematic and dynamic constraints depending on whether they significantly affect the type of motion being animated." Position, kinematic, balance (using ZMP), torque limit, and momentum constraints are all proposed as available constraints for this filter. The Kalman and least-squares filters converge to form the final motion. However, Tak states that "it is virtually impossible to characterize the analytical condition under which the repeated applications of the Kalman filter and least-square filter converge…[When] the editing involves dynamic constraints, we must deal with the velocities and accelerations, which are much more sensitive than positions." Though Tak's filter is able to create fantastic motions like dancing, wide stepping, golf swings, limbo walking, and jump kicks, the filtering methods use numeric filters and require iterative processing to create the stable filtered motion. Additionally, as Tak admits, there is not even a way to analytically determine how long it will take the filtering to converge, let alone create an analytical solution.

Yamane [38] describes a "dynamics filter, an online, full-body motion generator that converts a physically infeasible reference motion into a feasible one for the given human figure". The filter is able to account for collisions and contacts while creating a stable motion online, without prior knowledge of the rest of the motion. Reference motions that could be used include HMCD, motions created using animation software, or motions synthesized based on kinematics. The motion is generated based on an optimization scheme that computes joint values that satisfy the motion as well as dynamic constraints, which are expressed as constraints on the joint values. Contact and collisions are included in the filter using numeric trial and error procedures. Again, as Tak had expressed in his work, Yamane states that he could not find a systematic method for tuning the parameters for the filter. Both Tak and Yamane used numeric methods to filter motions and also could not determine a way to analytically describe the parameters used in the filters.

## 2 An AMF for humanoid robots

The Constrained Analytical Trajectory Filter is a component of an AMF described in [39,40]. The analytical solutions are faster than trial and error solutions and provide insights into the stability of the system that would otherwise be difficult to identify in a numeric optimization scheme. The resulting filtered motion should be as similar to the reference motion as possible while satisfying constraints. The definition of "similar" dictates the filtering methods used so as to achieve an optimum similarity. The AMF currently does not consider the physical limits of the actuators (torque, speed, etc.) or the possibility of link collisions. Additionally, it is assumed that the reference motion is possible for the robot to perform without violating the robot's kinematic and physical range of motion.

A typical humanoid robot has 20+ degrees of freedom (DOF). With so many DOF, analytical closed-form solutions are extremely difficult, if not impossible, to come by when

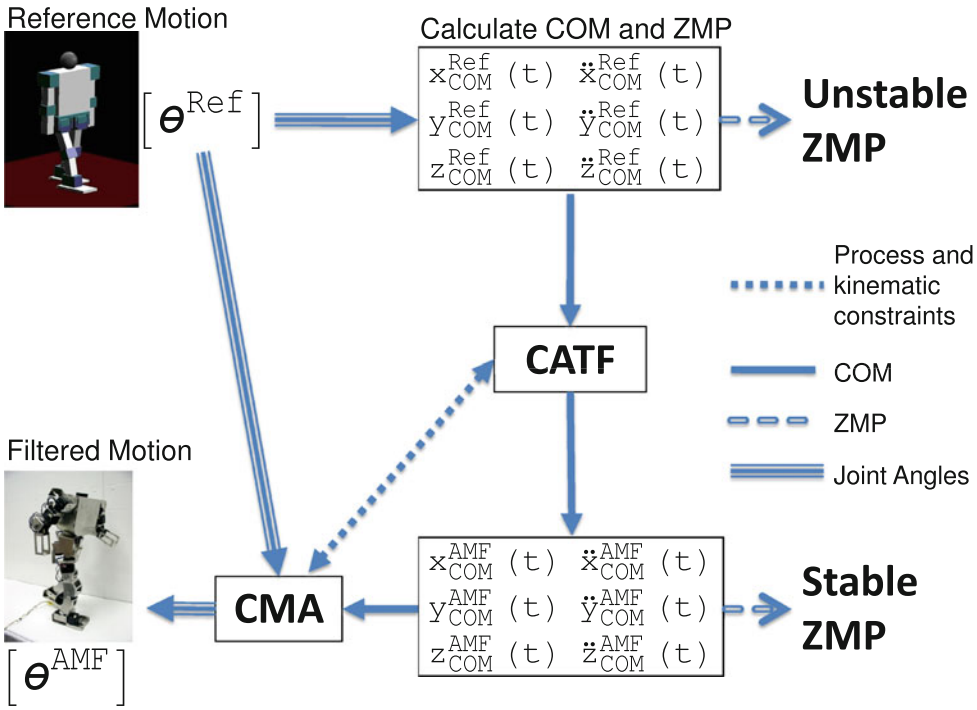


**Fig. 1** Flowchart outlining the Analytical Motion Filter (AMF)

generating stable walking gaits. This has given rise to many numeric brute force approaches that simply seek to solve an optimization function that includes stability in the cost function [7]. Instead of generating gaits blindly, the AMF approach generates and forms gaits based on closed-form analytical solutions that are based on ZMP stability. These solutions can be obtained from a high DOF system because the ZMP can be simplified to depend only on the three dimensional location of the center of mass (COM). Simplifying a 20+ DOF robot into a 3 DOF system allows for analytical closed-form solutions useful for creating stable motions [23]. The stability of the system then directly depends on the COM trajectory. The COM trajectory of a reference motion is easily calculated from the reference joint angles of the robot. However, instead of generating motions and gaits as Lim has, the analytical solutions in the AMF are used to modify the COM reference trajectory (Constrained Analytical Trajectory Filtering, CATF). The stability of the entire system can be guaranteed as long as the robot's kinematic and physical configuration allows it to follow the resulting stable COM trajectory. The modified stable COM trajectory is used in conjunction with the reference joint angles from the reference motion to determine what the new set of joint angles (AMF joint angles) need to be in order for the robot to have a stable motion (COM-based Motion Adaptation, CMA). Figure 1 illustrates the process for the AMF as described. During the entire process, the resulting filtered motion should be as similar to the reference motion as possible with differences minimized.

Once the CATF filters the reference COM trajectory, the result is what will be called the "AMF COM trajectory" (discussed in Sect. 3). Though it is straightforward to calculate the reference COM trajectory from the reference motion, which consists of joint angle trajectories, there are an infinite number of solutions to do the reverse–calculate the new AMF joint angle trajectories from the AMF COM trajectory. Calculating the new AMF joint angle trajectories (the AMF motion) is accomplished in the CMA. Since one of goals of the AMF is to try and minimize differences between the reference and filtered motion, calculating the *AMF* joint angle trajectories is accomplished using the *reference* joint angle trajectories as a starting point and deviating only enough to create a stable COM trajectory. When minimizing differences between the reference and AMF motion, the optimum solution depends on the definition of the difference between the reference and AMF motion. Hence, not only there are many different algorithms that could be used for calculating a set of joint angle trajectories from a COM trajectory, there are many different definitions of the cost function that relates changes from the reference motion to the filtered motion. Any number of algorithms could be used for the CMA, but the method used for the experiments in this work only modify the torso pitch and hip trajectory in the $X$–$Y$ plane when necessary. Figure 2 shows images of the robot pitching forward and back in order to allow the COM to follow the desired trajectory while minimizing changes in the trajectories of the joints in the lower body.


**Fig. 2** Video stills of a robot leaning back and forth to maintain stability by moving the COM location in the $X$-direction

## 3 Constrained Analytical Trajectory Filter approach

CATF is the portion of the AMF that takes a COM reference trajectory, which is calculated from the reference motion, and filters it so it is stable, creating the AMF filtered COM trajectory. Unstable motions are defined as those with a ZMP trajectory that goes outside of or to the edge of the support polygon. The ZMP is the stability criterion used in this work and is also the basis for the analytical solutions. In order to stabilize the reference motion, the CATF modifies the spatial and/or time information of the reference motion. The specifics for how the CATF modifies the reference motion depend on what characteristics of the reference motion are desired to carryover into the filtered motion, which are expressed as constraints. For example, if the robot's paths through space are paramount (i.e. when moving in a constrained space), then, if possible, the CATF will only modify the time/timing information of the motion, leaving the paths of the motion unchanged. This would involve either speeding up or slowing down the motion. Conversely, if the robot needs to appear to go through the same motion in the same amount of time, the CATF will only modify the spatial information of the COM reference trajectory, and only enough to stabilize the motion.

### 3.1 Stability

The analytical solutions and algorithms used in the CATF are derived and based on the stability of the robot. With a few exceptions (i.e. the Honda ASIMO, the Sony QRIO, the KAIST HUBO, and Tad McGeer's passive walker [27,25, 41–43]), most legged robots today walk using what is called the static stability criterion. The static stability criterion is an approach to prevent the robot from falling down by keeping the COM of its body over its support polygon by adjusting the position of its links and the pose of its body very slowly to minimize dynamic effects [27]. Thus, at any given instant in a statically stable motion, the robot could "pause" and not fall over. Statically stable walking is generally energy inefficient since the robot must constantly adjust its pose in such a way to keep the COM of the robot over its support polygon, which generally requires large torques at the joint actuators and/or awkward motions. Humans do not walk in this manner. Rather, we naturally walk dynamically, with the COM almost always outside our support polygon. Human walking can be interpreted as a cycle of continuously falling and recovering: a cycle of exchanging potential and kinetic energy in the system—much like the motion of a pendulum. We fall forward and catch ourselves with our swinging foot while continuing to walk forward. This falling motion allows for our COM to continually move forward and does not expend energy to stop the momentum. The lowered potential energy from this falling forward motion is then increased and recovered by the supporting leg lifting up the rest of our body.

One natural question that arises when examining dynamic walking is how to classify the gait's stability. Since the COM can travel outside of the support polygon, the static stability criterion is not useful. To address this, dynamic stability is commonly measured using the ZMP, which is a point defined as "where the influence of all forces acting on the mechanism can be replaced by one single force" without a moment term [44]. If this point remains in the support polygon, then the robot can apply some force or torque to the ground, which in turn means the robot can have some influence over the motion of itself (the system). Once the ZMP moves to the edge of the foot, the robot is unstable and can do nothing to recover without extending the support polygon (planting another foot or arm).

### 3.2 ZMP investigation

The equations governing the dynamic stability of a robot, the ZMP, are also what govern the solutions in this work. To explain how the solutions for this work were derived, we will start with the basic definition of the ZMP [44,45]. Using the axes from Fig. 3 and making assumptions that the angular accelerations are small or the moments of inertia are relatively small, the ZMP equation can be simplified, as many others have [15,17–20], and presented as:

$$x_{\text{ZMP}} = x_{\text{COM}} - \frac{\ddot{x}_{\text{COM}} \cdot z_{\text{COM}}}{\ddot{z}_{\text{COM}} + g} \tag{1a}$$

$$y_{\text{ZMP}} = y_{\text{COM}} - \frac{\ddot{y}_{\text{COM}} \cdot z_{\text{COM}}}{\ddot{z}_{\text{COM}} + g} \tag{1b}$$

where COM is the center of mass and $g$ is gravity. This simplification is representative of an inverted pendulum, which is often used for modeling bipedal robot gaits. An additional simplification can be made when $z_{\text{COM}}$ is relatively constant and $\ddot{z}_{\text{COM}}$ is relatively small compared to $g$:

$$x_{\text{ZMP}} = x_{\text{COM}} - \ddot{x}_{\text{COM}} \cdot H \tag{2a}$$

$$y_{\text{ZMP}} = y_{\text{COM}} - \ddot{y}_{\text{COM}} \cdot H \tag{2b}$$

where $H$ is $\frac{z_{\text{COM}}}{\ddot{z}_{\text{COM}}+g}$.

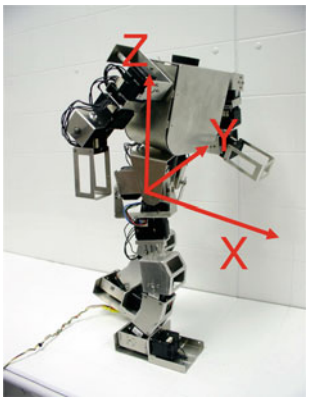


**Fig. 3** Diagram showing the axis labeling convention of a humanoid robot

### 3.3 Spatial scaling

The CATF can manipulate the COM trajectory in order to stabilize the reference motion while leaving the motion's time information (dimension) unchanged. For simplicity, only the process for filtering the $X$-direction will be shown in this section. The $x_{\text{ZMP}}$ and $y_{\text{ZMP}}$ are decoupled as seen in Eq. 1. The same process shown for the $X$-direction can be directly applied to the $Y$-direction without impacting stability in the $X$-direction, except for the cases of non-rectangular support polygons and when at kinematic extremes. Additionally, in keeping with the overall goal of the AMF, the COM trajectory is changed only as much as needed in order to achieve stability for the entire motion so as to reduce the differences between the filtered and reference motions.

The principle behind the spatial modification with the goal of achieving stability is to scale the COM trajectory down towards some nominally stable trajectory. To understand this concept, we first consider the motion of a robot standing perfectly still in a stable pose, which would result in COM path described as

$$x_{\text{COM}}(t) = D \tag{3}$$

where $x_{\text{ZMP}}^{\text{Low}} < D < x_{\text{ZMP}}^{\text{High}}$, and $D$ is a constant. Therefore, the $X$-acceleration is 0 and $x_{\text{COM}} = x_{\text{ZMP}}$. $x_{\text{ZMP}}^{\text{Low}}$ is the lower limit that the ZMP is permitted to be, which is usually the back of the robot's grounded foot. $x_{\text{ZMP}}^{\text{High}}$ is the upper limit that the ZMP is permitted to be, which is usually at the front of the robot's grounded foot. Since standing still with the COM within the support polygon (ZMP Limit) is inherently stable, scaling the reference COM trajectory down towards a constant position in the support polygon will eventually lead to a stable motion since accelerations will approach 0 as the trajectory starts resemble a constant and all of the COM positions approach the stable region. Using $x_{\text{ZMP}}^{\text{nom}}$, which is usually halfway between $x_{\text{ZMP}}^{\text{Low}}$ and $x_{\text{ZMP}}^{\text{High}}$ (or can be chosen elsewhere within the support polygon), the CATF scales the reference

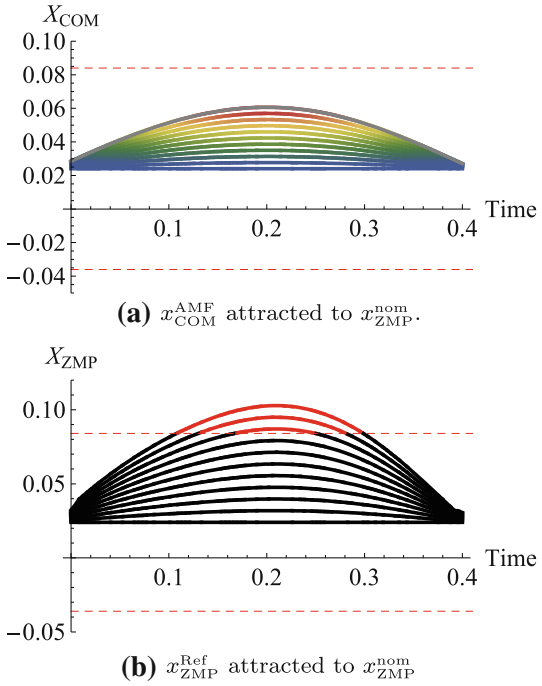


**(a)** $x_{\text{COM}}^{\text{AMF}}$ attracted to $x_{\text{ZMP}}^{\text{nom}}$.

**(b)** $x_{\text{ZMP}}^{\text{Ref}}$ attracted to $x_{\text{ZMP}}^{\text{nom}}$

**Fig. 4** Plots showing how $x_{\text{COM}}^{\text{AMF}}$ and $x_{\text{ZMP}}^{\text{Ref}}$ are attracted to $x_{\text{ZMP}}^{\text{nom}} = 0$ using Eq. 4. $C_s$ varies from 0 to 1 by increments of 0.1. The reference COM and ZMP trajectories are the most arched trajectories plotted. The dotted red lines represent the ZMP limits

motion down towards $x_{\text{ZMP}}^{\text{nom}}$ until the filtered motion is stable. The COM trajectory from the reference motion, $x_{\text{COM}}^{\text{Ref}}$, is scaled, resulting in the AMF COM trajectory defined as

$$x_{\text{COM}}^{\text{AMF}} = x_{\text{COM}}^{\text{Ref}} + C_s(x_{\text{ZMP}}^{\text{nom}} - x_{\text{COM}}^{\text{Ref}}) \tag{4}$$

which can create a stable, scaled-down version of the reference motion that centers around the nominal ZMP location, where $C_{\text{s}}$ is the spatial scaling factor and $x_{\text{COM}}^{\text{AMF}}$ is the filtered COM trajectory. Essentially, the COM trajectory is scaled so it is closer to the nominal ZMP value with smaller accelerations and $C_{\text{s}}$ dictating how much scaling is needed to stabilize the motion. Figure 4 helps to illustrate this process with a fabricated example reference motion. When $C_{\text{s}}$ is 0, $x_{\text{COM}}^{\text{AMF}} = x_{\text{COM}}^{\text{Ref}}$ and when $C_{\text{s}}$ is 1, $x_{\text{COM}}^{\text{AMF}} = x_{\text{ZMP}}^{\text{nom}}$. Again, because $x_{\text{COM}}^{\text{AMF}}$ is attracted to $x_{\text{ZMP}}^{\text{nom}}$ and the trajectory is "damped out," resulting in lower accelerations, the ZMP trajectory, $x_{\text{ZMP}}^{\text{AMF}}$, also approaches $x_{\text{ZMP}}^{\text{nom}}$.

If we define the greatest instability as the most reference ZMP trajectory, $x_{\text{ZMP}}^{\text{Ref}}$ leaves the ZMP range and denote it as $x_{\text{ZMP}}^{\text{err}}$, the motion can be stabilized using the scaling factor:

$$C_{\text{s}} = \frac{x_{\text{ZMP}}^{\text{err}}}{x_{\text{ZMP}}^{\text{nom}}(t_m) - x_{\text{ZMP}}^{\text{Ref}}(t_m)} \tag{5}$$

where $x_{\text{ZMP}}^{\text{nom}}$ is the nominal $x$ ZMP and $t_m$ is the time when $x_{\text{ZMP}}^{\text{Ref}}$ is the furthest from the ZMP range (or when $x_{\text{ZMP}}^{\text{err}}$ occurs—derivation can be found in [40]). Since $C_{\text{s}}$ scales the entire motion, it must be large enough to stabilize the most unstable

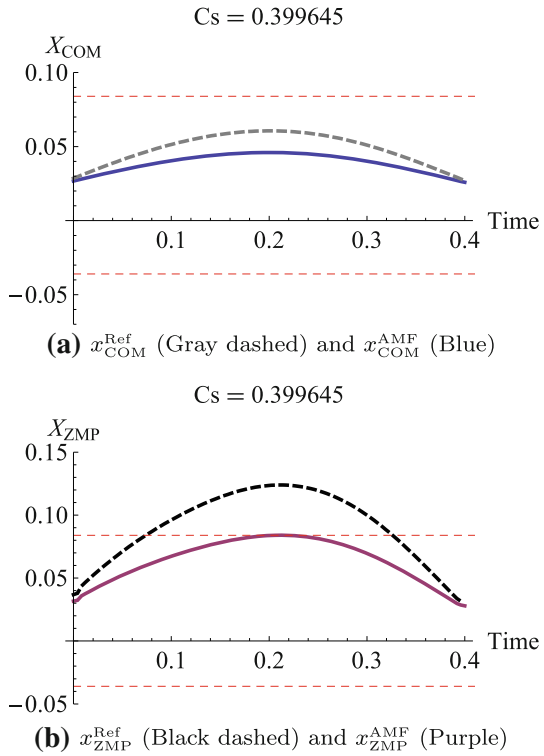


**(a)** $x_{COM}^{Ref}$ (Gray dashed) and $x_{COM}^{AMF}$ (Blue)

**(b)** $x_{ZMP}^{Ref}$ (Black dashed) and $x_{ZMP}^{AMF}$ (Purple)

**Fig. 5** Comparison of the reference and resulting filtered motion from spatial scaling. The red dashed lines are the ZMP limits

portion of the motion. If the most unstable portion of the motion is stabilized using this method, then any other areas of instabilities are consequently also stabilized. Using Eqs. 4 and 5, the example motion from Fig. 4 is filtered resulting in Fig. 5, which shows a comparison of $x_{COM}^{Ref}$ to the final stable $x_{COM}^{AMF}$. Additionally, since the resulting AMF COM trajectory is a scaled version of the reference COM trajectory, the motion naturally retains some characteristics of the reference COM trajectory, such as curve or shape. If handled appropriately in the CMA, the resulting AMF motion (including joint angle trajectories) can also result as a scaled version of the reference motion.

### 3.4 Time scaling

The compliment to scaling the spatial information of a motion would be to scale the time information of the motion—essentially slowing down or speeding up the motion. Leaving the spatial portion of the motion unchanged is a desirable feature in instances where path following is very important. Robots manipulating tools or navigating an obstruction may have to follow a very specific path in order to avoid collision, but the speed at which the task is accomplished may not be as important. One of the best features about only scaling the time information of the motion is that determining the joint angle trajectories for the filtered motion in the CMA is trivial—the joint angle trajectories maintain the same angular trajectories and inherit the same sort of "speeding up" or "slowing down" that the COM trajectory goes through in the CATF. The downside to modifying/scaling the time information is that the $X$ and $Y$ directions are inherently coupled—all spatial dimensions share the same time dimension. Therefore, it may be possible that speeding up or slowing down the motion may stabilize motion in the $X$-direction, but then destabilize motion in the $Y$-direction. Finally, in keeping with one of the overall goals of the AMF, the motion is only "sped up" or "slowed down" as much as needed in order to stabilize the motion so that differences between the reference and filtered motion are minimized.

We can describe speeding up or slowing down the reference motion, time scaling, as

$$x_{COM}^{AMF}(t) = x_{COM}^{Ref}(t') \tag{6a}$$

$$y_{COM}^{AMF}(t) = y_{COM}^{Ref}(t') \tag{6b}$$

where $t'$ is the new time information, which will be described as

$$t' = \int_0^t C(t)\,dt \tag{7}$$

where $C(t)$ describes the amount of "slowing down" or "speeding up" applied to the reference motion. From [40], the stability of the filtered motion can be shown as

$$x_{ZMP}^{AMF}(t) = x_{COM}(t') - H(\ddot{x}_{COM}(t')C^2(t) + \dot{x}_{COM}(t')C'(t)) \tag{8}$$

where $C'(t)$ is the derivative of $C(t)$ with respect to time. We can then rewrite the equation using discrete notation as

$$(x_{ZMP}^{AMF})_i = (x_{COM})_i - H((\ddot{x}_{COM})_i C_i^2 + (\dot{x}_{COM})_i C_i') \tag{9}$$

Since $C_i'$ is included in the solution, there is no clean way to solve for $C_i$. However, if $\dot{x}_{COM} = 0$ or $C_i' = 0$, then it is much simpler to find $C_i$. Since for most motions, $\dot{x}_{COM} \neq 0$, we hold $C_i$ as constant for the duration of the motion in order to obtain a solution for $C_i$.

$$(x_{ZMP}^{AMF})_i = (x_{COM})_i - H(\ddot{x}_{COM})_i C_i^2 \tag{10}$$

Therefore, if we say $C_i = C_T$ for the entire, motion, we can solve for $C_T$ as

$$C_T = \sqrt{\frac{(x_{COM})_\tau - x_{ZMP}^{Limit}}{H(\ddot{x}_{COM})_\tau}} \tag{11}$$

where $\tau$ occurs when $C_T$ is calculated as furthest from 1. $x_{ZMP}^{Limit}$ replaces $(x_{ZMP}^{AMF})_i$ since $C_T$ is designed to stabilize the motion just enough so that the ZMP is within the support polygon. Therefore, the most unstable point will lie on a ZMP limit. There are certain conditions that must exist in order for there to be a valid $C_T$ that can stabilize the reference motion since $C_i$ is constant for the entire motion. First, the result of (11)

must always be above or below 1 for all unstable portions of the motion. This is because if $C_T < 1$, the motion is slowed down and if $C_T > 1$, the motion is sped up. Since $C_i$ is constant, the entire motion can *only* be slowed down or sped up. Therefore, if part of the motion needs to be sped up in order to be stable and another part of the motion needs to be slowed, it is not possible to have a constant $C_i$ value. In order for this to be true, $x_{\mathrm{COM}}(t) - x_{\mathrm{ZMP}}^{\mathrm{Limit}} - H\ddot{x}_{\mathrm{COM}}(t)$ must be either greater than or less than zero for all unstable portions of the reference motion (solved by setting $C_T = 1$ in Eq. 11).

Holding $C_i$ constant presents additional constraints on what motions can be stabilized from scaling the time information. Given Eqs. 11 and 2, three cases of instability can occur with respect to the speed of the motion:

1. $x_{\mathrm{COM}}^{\mathrm{Ref}}$ is over the support polygon, and therefore within the ZMP range, but the magnitude of $\ddot{x}_{\mathrm{COM}}^{\mathrm{Ref}}$ is too high and causes instability by pushing $x_{\mathrm{ZMP}}^{\mathrm{Ref}}$ outside of the ZMP limit.
2. $x_{\mathrm{COM}}^{\mathrm{Ref}}$ is outside of the support polygon and the sign of $\ddot{x}_{\mathrm{COM}}^{\mathrm{Ref}}$ is the opposite of $x_{\mathrm{ZMP}}^{\mathrm{Ref}} - x_{\mathrm{ZMP}}^{\mathrm{Range}}$. Instability occurs because $\ddot{x}_{\mathrm{COM}}^{\mathrm{Ref}}$ is not the correct magnitude.
3. $x_{\mathrm{COM}}^{\mathrm{Ref}}$ is outside of the support polygon and the sign of $\ddot{x}_{\mathrm{COM}}^{\mathrm{Ref}}$ is the same as the sign of $x_{\mathrm{ZMP}}^{\mathrm{Ref}} - x_{\mathrm{ZMP}}^{\mathrm{Range}}$. Instability is guaranteed no matter how fast or slow the motion is.

Case 1 is the simplest case to understand. If $x_{\mathrm{COM}}^{\mathrm{Ref}}$ is over the support polygon, the robot can be stable if the motion slows down and takes an infinite amount of time to occur, which drives the COM acceleration to zero. The resulting ZMP then coincides with the COM, which is over the support polygon and therefore stable.

Case 2 highlights the relationship between the COM position and the COM acceleration. If $x_{\mathrm{COM}}^{\mathrm{Ref}}$ is above $x_{\mathrm{ZMP}}^{\mathrm{High}}$, the acceleration must be positive (since $H > 0$ in Eq. 2) in order for the resulting ZMP, $x_{\mathrm{ZMP}}^{\mathrm{Ref}}$, to be under $x_{\mathrm{ZMP}}^{\mathrm{High}}$. Likewise, the acceleration must be negative if the COM position is below $x_{\mathrm{ZMP}}^{\mathrm{Low}}$ in order for Case 2 to occur. Adjusting the speed of the reference motion can result in a stable motion by changing the magnitude of the acceleration and bringing the ZMP within limits. In this case, stabilizing the motion may involve either speeding up or slowing down the motion.

Cases 2 and 3 are opposite to each other; Case 2 can be stabilized while Case 3 cannot. If the COM position is above $x_{\mathrm{ZMP}}^{\mathrm{High}}$ and the COM acceleration is negative, it does not matter how much faster or slower the motion is, there is no magnitude of the acceleration that would yield a ZMP below $x_{\mathrm{ZMP}}^{\mathrm{High}}$. The same situation occurs if the COM is below $x_{\mathrm{ZMP}}^{\mathrm{Low}}$ and the COM acceleration is positive. This presents an interesting characteristic that was not present in spatial scaling. When scaling the spatial dimensions of the reference motion, there was always a stable solution. However, when only scaling the time dimension of the motion, it is possible that the motion

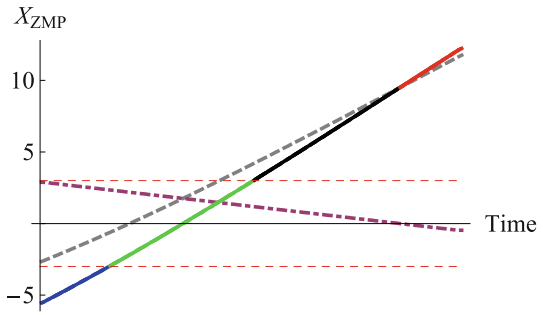


**Fig. 6** $x_{\mathrm{COM}}^{\mathrm{Ref}}$ (Dashed gray), $\ddot{x}_{\mathrm{COM}}^{\mathrm{Ref}}$ (Dot-dashed purple), $x_{\mathrm{ZMP}}^{\mathrm{Ref}}$: Categorized by instability; black is Case 1, blue is Case 2, red is Case 3, and green is stable. $H = 1$ for this example

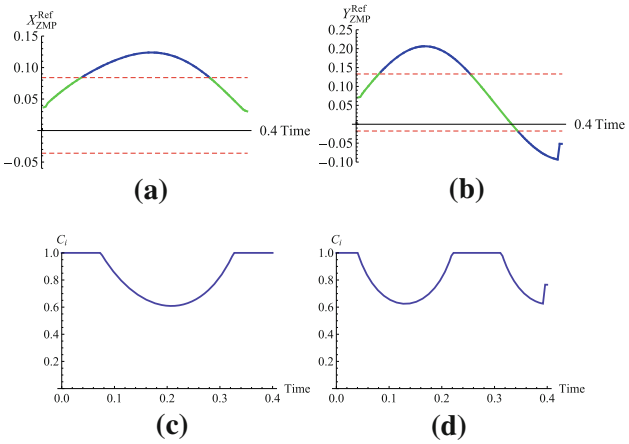


**Fig. 7** Fabricated sample reference motion. ZMP plots: $\ddot{x}_{\mathrm{ZMP}}^{\mathrm{Ref}}$: Categorized by instability; blue is Case 2 and green is stable. And then corresponding $C_i$ plots

cannot be stabilized. An easy example to visualize this case would be if a robot was holding a very heavy weight beyond the front of its feet while stepping backwards; no matter how quickly or slowly the robot steps backwards, it will fall over towards its front.

Figure 6 shows a plot of a fabricated sample reference motion. The different types of instability can be seen along with the corresponding reference motion and reference motion acceleration.

As an example to show how changing the speed of the reference motion can stabilize the motion, Fig. 7 shows ZMP trajectories in the $X$ and $Y$ directions with their instabilities classified. Also shown are the corresponding $C_i$ values calculated using (11) for each instance. As seen, $C_i$ is calculated as constantly below 1 and no Case 3 instabilities are present. Since $C_i$ is held constant, the most extreme $C_i$ value is used first for each direction to show the effect of speeding up and slowing down the reference motion as seen in Fig. 8.

Since the $X$ and $Y$ directions are coupled, only one $C_T$ value can be used. Again, the most extreme $C_T$ value between the two directions is used. Since it is possible that the speeding

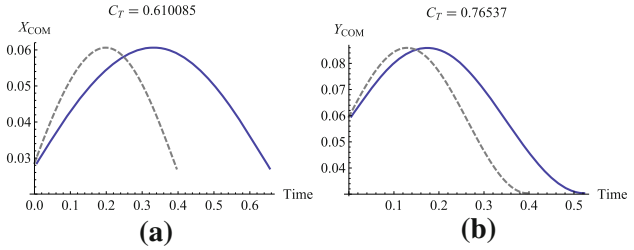


**Fig. 8** Resulting COM trajectories from slowing down the motion by the factor $C_T$ calculated for each direction independently. $x_{COM}^{Ref}$ (Gray dashed) and $x_{COM}^{AMF}$ (Blue)

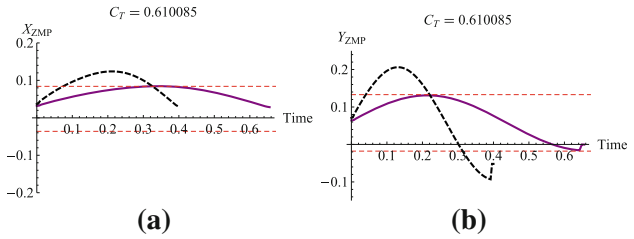


**Fig. 9** Resulting ZMP trajectories from slowing down the motion by the factor $C_T$. $x_{ZMP}^{Ref}$ (Black dashed) and $x_{ZMP}^{AMF}$ (Purple)

up or slowing down the motion in one direction could destabilize the other direction, we must check the $C_T$ value used in both directions. Figure 9 shows the resulting AMF ZMP trajectories using the same and most extreme $C_T$ value applied to slow down the motion. As seen, the ZMP trajectories in both direction remain within the support polygon, and though while difficult to see, the $Y$-direction is over-stabilized since it is slowed more than necessary for a stable ZMP path.

## 4 Experiments and results

Spatial and time scaling were applied to a walking gait and circular motion in both simulation and on actual hardware. The test platform used was the Dynamic Anthropomorphic Robot with Intelligence (DARwIn, Fig. 10), a humanoid robot developed at the Robotics and Mechanisms Laboratory (RoMeLa). DARwIn is primarily used as a research tool for studying bipedal and humanoid locomotion, but was also used in the autonomous robot soccer competition, RoboCup.

### 4.1 Walking gait

The piecewise gait is very common type of walking gait used that is based on trajectory following. The gait is divided into (sometimes arbitrary) portions so that the gait is defined with different equations for each portion. Typically, the hip/pelvis and ankle trajectories are the only defined trajectories from the equations. Inverse kinematics are used to derive all of the joint angles. The piecewise gait developed by Qiang was designed to be used in a numeric optimization scheme.

The equations governing the gait are described in [7]. The described gait is only a 2D planar gait—not considering the $Y$-direction of the robot. The $Y$-direction trajectories were generated using polynomial fits for this example.

Table 1 shows the values used for generating the gait for this example case.

Even though the gait was modified to be unstable, the robot still does not fall over while walking. Figure 11 shows two pictures of Qiang's piecewise gait from the rear view. The gait is designed such that the upper body and hips are perfectly level throughout the entire motion. As seen, the robot leans significantly to each side as it steps. This leaning occurs because the motors used in the test platform, DARwIn, use a


**Fig. 10** DARwIn III test platform

**Table 1** Input gait parameters used for Qiang's piecewise gait

| Description | Variable | Value (metric) |
|---|---|---|
| Step time | $T_c$ | 1 (s) |
| Double support time | $T_D$ | 0 (s) |
| Time at step height | $T_m$ | 0.5 (s) |
| Step length | $D_s$ | 0.10 (m) |
| Angle of ankle | $q_*$ | 0 (rad) |
| Midway step length | $L_{ao}$ | 0 (m) |
| Step height | $H_{ao}$ | 0.025 (m) |
| Minimum hip height | $H_{hmin}$ | 0.20 (m) |
| Maximum hip height | $H_{hmin}$ | 0.21 (m) |

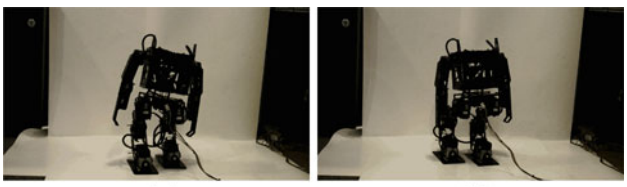


**Fig. 11** Video stills of the Qiang's piecewise reference gait that show the robot leaning

proportional position controller. Therefore, high loads on a motor cause large errors. During SSP, very large torques are need from the motors to keep the robot from leaning. As seen, the proportional controller is not enough and the robot is able to lean, which actually keeps it from falling over. Though for this gait, the robot's leaning kept it stable and from falling over, in all of the other walking gaits, this error proves to destabilize even a stable motion.

Therefore, experiments for the walking gaits applied to the robot hardware were inconclusive due to the system's compliance. In order to validate the CATF outside of simulation and on actual hardware, a circular sway motion was used (as discussed in Sect. 4.2). The circular sway motion is stationary (not walking), and therefore the torques required from the motors are not as high and the joint angle error is significantly reduced.

### *4.1.1 Resulting reference COM and ZMP trajectory*

The results for the COM reference trajectory can be seen in Fig. 12. Also seen are the COM limits enforced by kinematic constraints. The range of the COM in the $X$-direction is dictated by how far forward and back the waist of the robot can move since it will be used as the primary means of modifying the COM position in the CMA when generating the filtered joint angles. The range of the COM in the $Y$-direction, which is dictated by kinematic constraints, is very large because the height of the robot is relatively low, allowing for a large range of travel of the hip.

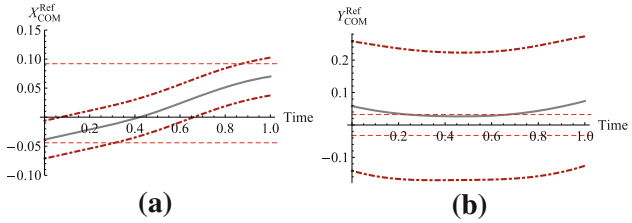


**Fig. 12** COM reference trajectories for Qiang's piecewise gait. Reference trajectory shown as solid gray and the kinematic limits of the COM are shown as dot dashed dark red

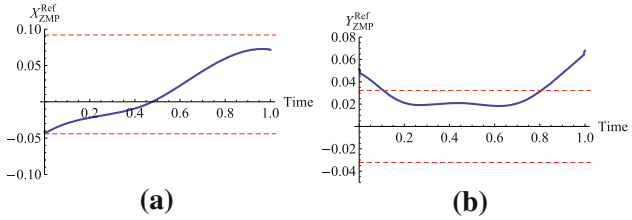


**Fig. 13** ZMP reference trajectories for Qiang's piecewise gait

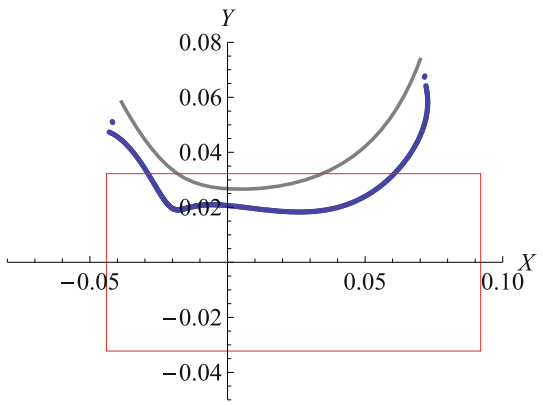


**Fig. 14** COM (Gray) and ZMP (Blue) reference trajectories for Qiang's piecewise gait. The red box represents the support polygon

The results for the ZMP reference trajectory can be seen in Fig. 13. As seen, only the $Y$-direction of the motion has unstable portions. Figure 14 shows a parametric plot of both the reference COM and ZMP.[1] It is clear that the $Y$-direction of the motion is largely unstable at the beginning and end of the motion.

### *4.1.2 Simple time scaling*

In order to determine if time scaling is feasible, the CATF analyzes the motion to determine what cases of instability occur as described in Sect. 3.4. Figure 15 shows that the

[1] The ZMP points that do not line up smoothly with the rest of the motion (also seen in Fig. 13b) are a result of inaccurate estimations of the acceleration of the COM at the beginning and ends of the motion. Since motion data are not available beyond those points, the acceleration calculations are a little off.

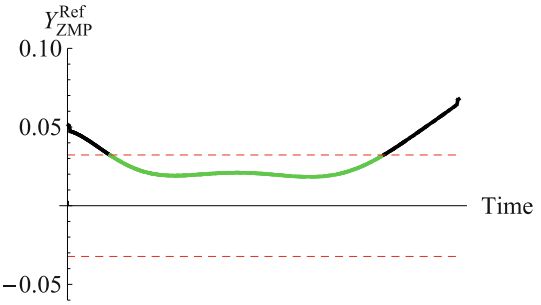


**Fig. 15** Categorized instability for Qiang's piecewise gait. Black is Case 1, and Green is Stable

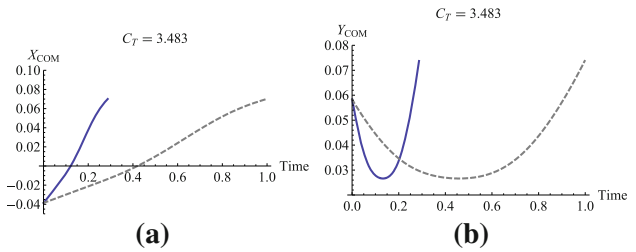


**Fig. 16** AMF COM trajectories from using time scaling on Qiang's piecewise gait. Reference COM is dashed gray and AMF COM is solid blue

$Y$-direction has no Case 3 instabilities. Therefore, it may be possible to stabilize the gait simply by slowing it down or speeding it up. However, notice that the ZMP in the $X$-direction is very close to the edge of the support polygon at the beginning of the motion. This area could potentially destabilize if the motion's speed is changed.

Figure 16 shows the result of using Eq. 10. As seen, the motion is sped up; a duration of 0.29 s compared to 1.0 s for the reference motion. Since it is possible that in speeding up the motion and stabilizing the most unstable portion of the reference motion in the $Y$-direction, other parts of the motion were destabilized, it is important to check the resulting ZMP. Figure 17 shows the resulting ZMP in both directions. As seen, though speeding up the entire motion may have stabilized the very beginning and end of the motion in the $Y$-direction, many other parts of the motions in the $Y$-direction were destabilized. Not only is the $Y$-direction unstable, but the $X$-direction as well. Therefore, simple time scaling cannot be used to stabilize this motion.

## 4.2 Circular sway

A simple non-walking motion such as a robot swaying in a circle (much like when using a hoola-hoop) can demonstrate the majority of the capabilities of the AMF. The hips follow a cyclic circle trajectory while the upper body is motionless.

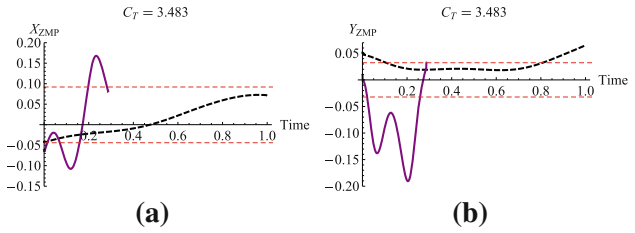


**Fig. 17** AMF ZMP trajectories from using time scaling on Qiang's piecewise gait. Reference ZMP is dashed black and AMF ZMP is solid purple

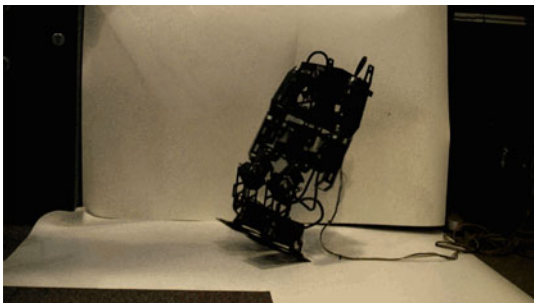

**Fig. 18** Picture of DARwIn falling over while trying to perform the reference circular gait on a high friction surface

### 4.2.1 Equations governing reference motion

The circular sway gait is very simple. The hips move in a circular motion and the feet do not leave the ground. The motion is described as

$$\text{Hip}_x(t) := 0.04\sin(2\pi t) + 0.02 \tag{12a}$$

$$\text{Hip}_y(t) := 0.04\cos(2\pi t) \tag{12b}$$

$$\text{Hip}_z(t) := 0.23 \tag{12c}$$

and $T_s = 0.5$.

Figure 18 shows a picture of the robot attempting to perform the reference circular gait on a surface with a relatively high coefficient of friction. The instability is very clear as the robot falls over almost immediately after attempting to perform the gait. Figure 19 shows a picture of the robot attempting to perform the reference circular gait on a surface with a relatively low coefficient of friction. The robot does not fall over, but tips up on the edges of both its feet.

### 4.2.2 Resulting reference COM and ZMP trajectory

The results for the COM reference trajectory can be seen in Fig. 20. Also seen are the COM limits enforced by kinematic constraints. The range of the X-COM is dictated by how far forward and back the waist of the robot can move since it will be used as the primary means in the CMA when generating the filtered joint angles. The range of the Y-COM coincidentally follows the Y-COM trajectory, but is calculated based

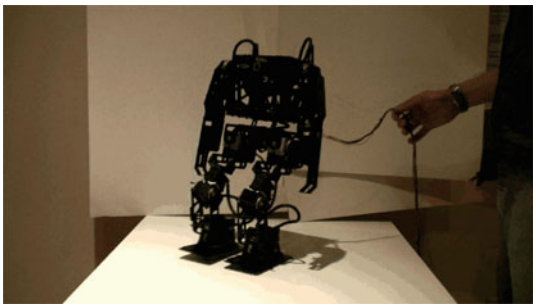

**Fig. 19** Picture of DARwIn tipping while trying to perform the reference circular gait on a low friction surface

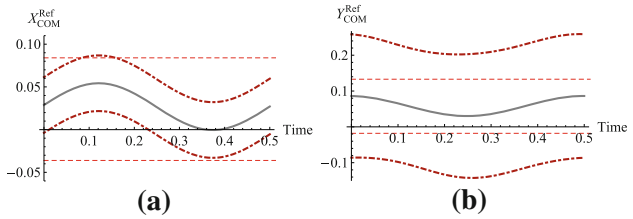


**Fig. 20** COM reference trajectories for a circular sway motion. Reference trajectory shown as solid gray and the kinematic limits of the COM are shown as dot dashed dark red

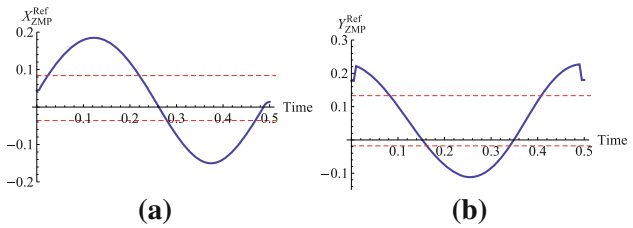


**Fig. 21** ZMP reference trajectories for a circular sway motion

on the kinematic limitations of the robot. While maintaining the same hip height and X-COM location, the hips can only go so far in the $Y$-direction based on the link lengths of the legs.

The results for the ZMP reference trajectory can be seen in Fig. 21. As seen, both the $X$ and $Y$ directions of the motion have unstable portions. Figure 22 shows a parametric plot of both the reference COM and ZMP trajectories.[2] It is clear that circular sway motion is largely unstable, with the ZMP always outside of the support polygon.

### *4.2.3 Simple spatial scaling*

The solutions from Sect. 3.3 are applied to both $X$ and $Y$ directions of the reference motion in order to stabilize the

[2] The ZMP points that do not line up smoothly with the rest of the motion (also seen in Fig. 21) are a result of inaccurate estimations of the acceleration of the COM at the beginning and ends of the motion. Since motion data are not available beyond those points, the accelerations calculations are a little off.

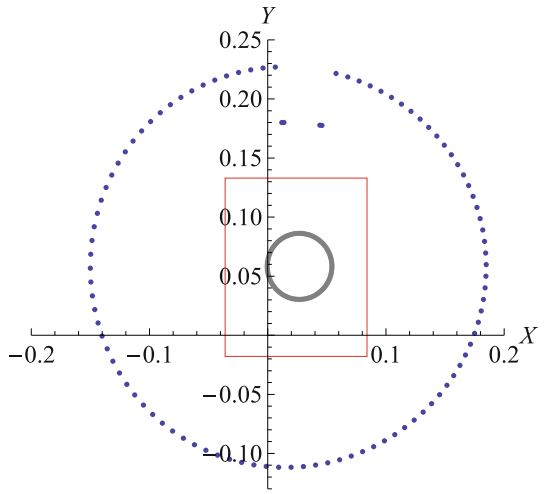


**Fig. 22** COM (Gray) and ZMP (Blue) reference trajectories for a circular sway gait. The red box represents the support polygon

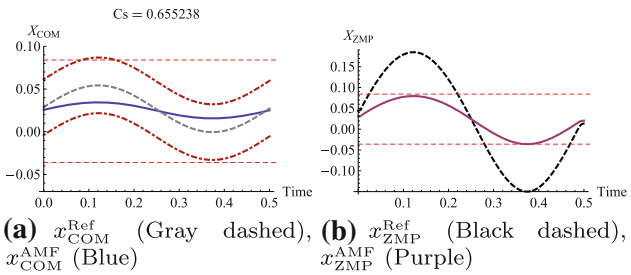


**Fig. 23** AMF $X$-direction trajectories from spatial scaling using the circular sway gait

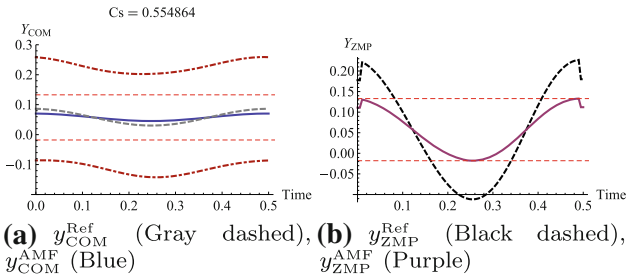


**Fig. 24** AMF $Y$-direction trajectories from spatial scaling using the circular sway gait

motion. Since there is no walking or changing of ground contact, simple spatial scaling makes sense as a way to stabilize the gait while retaining characteristics of the reference gait such as shape, timing, etc. As seen in Figs. 23 and 24, the CATF scales the COM motion just enough to create a stable motion. The reference and filtered COM trajectories maintain similar characteristics of shape.

The damped out motion should result in the waist pitching in the opposite direction that the rest of the robot is moving. Additionally, the hips of the robot should not be moving as much laterally as in the reference motion. Figure 25 shows

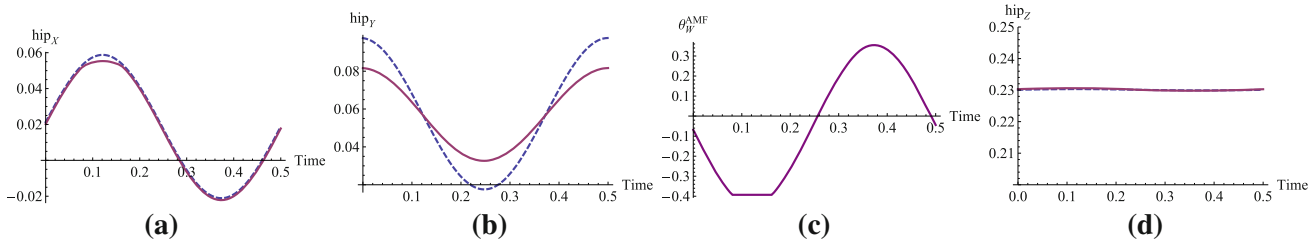


**Fig. 25** Resulting AMF motion after applying the CMA to the circular sway gait that was stabilized using simple spatial scaling by the CATF. Reference motion is dashed blue and the AMF motion is solid purple

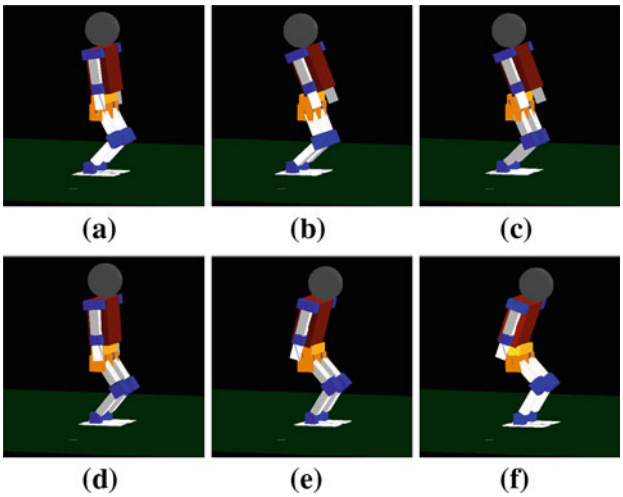


**Fig. 26** Simulation stills of the AMF solution using spatial scaling applied to the circular sway gait

the resulting changes in the hip trajectory and waist angle trajectory. As seen, the waist cannot completely move the COM in the $X$-direction to satisfy the AMF trajectory without hitting the limit of $\pi/8$. Therefore, at the clipped portions of the waist angle trajectory, the location of the hip in the $X$-direction slightly deviates from the reference trajectory in order to locate the COM. Additionally, in the filtered version of the motion, hips do not have as large an amplitude in the $Y$-direction; the motion damped out. Finally, there was very little change in the vertical location of the COM after changing the waist angle and hip locations. This makes sense since the waist at an angle of $\pi/8$ only changes the vertical location of the COM by about 3%.[3] Figure 26 shows a sequence of still shots of the filtered gait in simulation. The pitching of the torso is the most noticeable difference when comparing the filtered motion against the reference motion. However, if the upper body motion is not important with respect to the importance of the lower body motion, then it is perfectly acceptable to have the upper body pitching if it means the lower body motion remains relatively unchanged.

[3] Change in height of the torso's mass is $1 - \cos(\pi/8) = 7.6\%$. Additionally, the torso is only 38.6% of the total mass of the robot. Therefore, $7.6\% \cdot 38.6\% = 2.93\%$ for the total percent change in height.

## 5 Discussion and conclusions

The work presents the Constrained Analytical Trajectory Filter as a component of an AMF that creates a stable motion from a reference motion for humanoid robots. The CATF (Sect. 3) used the resulting COM trajectory from the reference motion as a representation of the motion as a whole. Using the COM trajectory, the ZMP trajectory, which measures the stability of the robot (Sect. 3.2), indicates which portions of the motion are unstable. Additionally, during investigation of these instabilities, it was discovered there were actually different kinds of instabilities (Sect. 3.4). The different cases of instability gave more insight as to why a particular motion was unstable: the motion was too fast, too slow, or inherently unstable. Two primary means of stabilizing a gait were utilized: time and spatial scaling. Spatial scaling scaled the COM trajectory down towards a known stable trajectory. Time scaling worked similarly by changing the speed of the motion, but was limited in effectiveness based on the types of instabilities in the motion and the coupling of the $X$ and $Y$ directions.

During investigation of spatial scaling, it was soon realized that the kinematic limitation of the robot had to be taken into consideration since an arbitrary COM trajectory cannot be created and followed by the robot. Therefore, the reference motion's joint angle trajectories in combination with the methods used in the CMA dictated the limitations on where the COM could exist after finishing filtering in the CATF. Generally, the kinematic constraints are not a problem since the motion is scaled to a stable trajectory, which is typically further from any kinematic limit than the reference motion. However, by considering kinematic limits, the nominal ZMP or amount of spatial scaling could be adjusted such that kinematic constraints were not violated in the CMA when satisfying the filtered COM trajectory.

Both time and spatial scaling have limitation or constraints to satisfy that are inherent in the system. Conversely, they

both have extremely attractive advantages over the other. Time scaling does not have to consider kinematic constraints or limitations since the COM path through space is unchanged and therefore the joint angle trajectories unchanged. Since the joint angles of the filtered motion are the same as the reference motion, and the reference motion is assumed to be kinematically feasible, the resulting joint angles for time scaling are naturally feasible. However, time scaling is ineffective for certain portions of motion that are inherently unstable, which is where the strength of spatial scaling is realized. While spatial scaling can potentially stabilize any reference motion, it must consider and follow kinematic constraints since the resulting COM path must be kinematically feasible.

No aspect of the CATF or AMF currently considers loading on the robot's joints or collision between robot links. Collision between robot links could be expressed as kinematic constraints, but could prove cumbersome. Torques, speeds, and accelerations of joints are not analyzed in this work. Therefore, the AMF, as it is now, could potentially generate a motion that requires unreasonably high speeds or torques from the joint actuators. Even though the motion may be theoretically stable, the robot could still not be able to perform the motion. A similar situation occurs if the AMF motion has joints colliding. When deriving the ZMP equations in Sect. 3.2, many researchers assume the robot's moments of inertia to be relatively small (especially when considering smaller humanoid robots). Large moments of inertia or angular accelerations could invalidate some of the assumptions. The errors caused by these assumptions can be mitigated by creating a factor of safety and keeping the ZMP well within the support polygon.

In this work, time scaling was simplified such that the time scaling was constant in order to simplify and generate a solution in Sect. 3.4. However, it would be very interesting to see in future work the inclusion of a time-varying time scaling function as shown in Eq. 9. Using a time-varying function, time scaling could stabilize many more gaits—including those with Class 3 instabilities. Additionally, a varying time scale function can allow additional constraints on the motions, such as a time step constraint. With a constant time scaling function, the duration of the motion is changed; however, a changing function could allow for time lost or gained in stabilizing unstable portions of the motion to be "made up" by doing the opposite, slowing down or speeding up, in the stable portions of the motion. Finally, a time-varying function may also allow for a more direct way to determine the optimal speeds of the entire motion in order to stably complete the motion as quickly as possible. An obvious benefactor would be robots in automation tasks in industry. If industry decides to use humanoid robots or robots that use the ZMP as stability criteria, it would be very beneficial to have a closed-form solution to determine the fastest way to follow a potentially unstable path through space.

During the experiments with the physical hardware, it was obvious that the robot platform was not sufficient for some gaits. The servo motors used to control the joints of the robot use a simple proportional position controller, which means that there will always be error in the joint angles–even more error for higher loads. Therefore, especially for the SSP of the walking gaits where loads were very high on some of the joints and actuators, the robot did not follow the joint angle trajectories closely. Even if the generated joint angle trajectories produce a stable walking motion in simulations, the motors do not precisely follow the trajectories to implement the gait. Future work should include either a reevaluation of the robot hardware or work on a control to compensate for the joint angle errors created at the joints.

Moving the COM by changing the joint angle trajectories in order to stabilize a gait can be effective; however, it could generally be inefficient. If a robot is constantly bending forward or leaning in one direction in order to create a stable gait, it may be more worthwhile to redesign the robot–or at least the mass distribution of the robot. Incorporating mass distribution and the robot's physical design into the motion filter could be very valuable in understanding the relationship between gait stability and walking platforms. Determining the physical design of a robot necessary to precisely and stably mimic a human's walking motion would not only be a fantastic advancement for robotics, but also for understanding the dynamic relationship between humans and robots.

The Constrained Analytical Trajectory Filter presented in this work lays out some foundations for further investigating the complex interactions between the COM trajectory and gait stability of a humanoid robot. The algorithms used in this work could also be expanded to legged robots or entirely different platforms that depend on stability and can use the ZMP as a stability criterion. One of the primary contributions of this work was showing that an entire reference motion could be stabilized using a single set of closed-form solutions and equations. Previous work by others considered optimization functions and numeric schemes to stabilize all or a portion of a gait. Instead, the CATF as part of the AMF gives a direct relationship between the input reference motion and the resulting filtered output motion.

**Acknowledgments** The authors would like to recognize the National Science Foundation and the Office of Naval Research for partially supporting this work through grants OISE 0730206, CNS 0960061, CNS 0958406, and ONR 450066.

## References

1. Anderson FC, Pandy MG (2001) Dynamic optimization of human walking. J Biomech Eng 123(5):381–390. doi:10.1115/1.1392310, http://link.aip.org/link/?JBY/123/381/1

2. Behnke S (2006) Online trajectory generation for omnidirectional biped walking. In: Proceedings of the 2006 IEEE international conference on robotics and automation, ICRA 2006, May 15–19, 2006, Orlando, FL, USA, pp 1597–1603
3. Bessonnet G, Chessé S, Sardain P (2004) Optimal gait synthesis of a seven-link planar biped. Int J Robotic Res 23(10–11):1059–1073
4. Bessonnet G, Seguin P, Sardain P (2005) A parametric optimization approach to walking pattern synthesis. Int J Robotics Res 24(7):523–536
5. Chevallereau C, Aoustin Y (2001) Optimal reference trajectories for walking and running of a biped robot. Robotica 19(5):557–569. doi:10.1017/S0263574701003307
6. Huang Q, Kajita S, Koyachi N, Kaneko K, Yokoi K, Arai H, Komoriya K, Tanie K (1999) A high stability, smooth walking pattern for a biped robot. In: ICRA, p 65
7. Huang Q, Yokoi K, Kajita S, Kaneko K, Arai H, Koyachi N, Tanie K (2001) Planning walking patterns for a biped robot. IEEE Trans Robotics Autom 17(3):280–289. doi:10.1109/70.938385
8. Hu L, Zhou C, Sun Z (2006) Biped gait optimization using spline function based probability model. In: Proceedings of the 2006 IEEE international conference on robotics and automation, ICRA 2006, May 15–19, 2006, Orlando, FL, USA, pp 830–835
9. Capi G, Nasu Y, Barolli L, Mitobe K (2003) Real time gait generation for autonomous humanoid robots: a case study for walking. Robotics Auton Syst 42(2):107–116. http://dblp.uni-trier.de/db/journals/ras/ras42.html#CapiNBM03
10. Capi G, Nasu Y, Barolli L, Mitobe K, Takeda K (2001) Application of genetic algorithms for biped robot gait synthesis optimization during walking and going up-stairs. Adv Robotics 15(6):675–694
11. Kim D, Kim N, Seo S, Park G (2005) Use of fuzzy system in modeling of biped walking robot. Int J Knowl-Based Intell Eng Syst 9(4):341–349
12. Kim D, Seo SJ, Park GT (2005) Zero-moment point trajectory modelling of a biped walking robot using an adaptive neuro-fuzzy system. IEE Proc Control Theory Appl 152(4):411–426. doi:10.1049/ip-cta:20045007
13. Dasgupta A, Nakamura Y (1999) Making feasible walking motion of humanoid robots from human motion capture data. In: Proceedings of the international conference on robotics and automation, pp 1044–1049
14. Buczek F, Cooney K, Walker M, Rainbow M, Concha M, Sanders J (2005) Performance of an inverted pendulum model directly applied to normal human gait. Clin Biomech 21:288–296
15. Kajita S, Kanehiro F, Kaneko K, Fujiwara K, Yokoi K, Hirukawa H (2003) Biped walking pattern generation by a simple three-dimensional inverted pendulum model. Adv Robotics 17(2):131–147
16. Sugihara T, Nakamura Y (2003) Contact phase invariant control for humanoid robot based on variable impedant inverted pendulum model. In: Proceedings of IEEE international conference on robotics and automation, ICRA '03, vol 1, p 51
17. Zhu C, Tomizawa Y, Luo X, Kawamura A (2004) Biped walking with variable zmp, frictional constraint, and inverted pendulum model. In: Proceedings of the international conference on robotics and biomimetics, pp 425–430
18. Zhu C, Kawamura A (2003) Walking principle analysis for biped robot with zmp concept, friction constraint, and inverted pendulum. In: Proceedings of the international conference on intelligent robots and systems, pp 364–369
19. Morisawa M, Kajita S, Kaneko K, Harada K, Kanehiro F, Fujiwara K, Hirukawa H (2005) Pattern generation of biped walking constrained on parametric surface. In: Proceedings of the international conference on robotics and automation, pp 2405–2410
20. Kajita S, Kaneko K, Harada K, Kanehiro F, Fujiwara K, Hirukawa H, Yokoi K (2003) Biped walking pattern generation by using preview control of zero-moment point. In: Proceedings of the international conference on robotics and automation, pp 1620–1626
21. Takanishi A, ok Lim H, Tsuda M, Kato I (1990) Realization of dynamic biped walking stabilized by trunk motion on a sagittally uneven surface.In: Proceedings of IROS 1990 IEEE international workshop on intelligent robots and systems, vol 1, pp 323–330
22. Lim S (2007) Dynamic stair walking of biped humanoid robots. J Mech Sci Technol 21(6):970–975
23. Lim S, KIM K, Son Y, Kang H (2005) Walk simulations of a biped robot. In: Proceedings of the international conference on control, automation, and systems
24. Muecke K, Hong D, Lim S (2008) Precision circular walking of bipedal robots. ASME/IDETC/CIE
25. McGeer T (1990) Passive dynamic walking. Int J Robotics Res 9(2):62–82. doi:10.1177/027836499000900206
26. McGeer T (1990) Passive walking with knees. In: Proceedings of the IEEE international conference on robotics and automation, vol 3, pp 1640–1645. doi:10.1109/ROBOT.1990.126245
27. Kim J (2006) On the stable dynamic walking of biped humanoid robots. PhD Thesis. Korea Advanced Institute of Science and Technology, Daejeon, South Korea
28. Kim J, Park I, Oh J (2006) Experimental realization of dynamic walking of the biped humanoid robot khr-2 using zero moment point feedback and inertial measurement. Adv Robotics 20(6):707–736
29. Kim J, Oh J (2004) Realization of dynamic walking for the humanoid robot platform khr-1. Adv Robotics 18(7):749–768
30. Lee J, Park I-W JL, Kim J-Y, Oh JH (2006) Online free walking trajectory generation for biped humanoid robot khr-3 (hubo). In: Proceedings of the IEEE international conference on robotics and automation, pp 1231–1236
31. Lee BJ, Kim YD, Kim JH (2004) Balance control of humanoid robot using its upper body. In: Proceedings of the 2004 FIRA robot world congress
32. Park JH (2001) Impedance control for biped robot locomotion. IEEE Trans Robotics Autom 17(6):870–882. doi:10.1109/70.976014
33. Huang Q, Nakamura Y (2005) Sensory reflex control for humanoid walking. IEEE Trans Robotics 21(5):977–984. doi:10.1109/TRO.2005.851381
34. Popovic Z (2000) Editing dynamic properties of captured human motion. In: Proceedings of the international conference on robotics and automation, vol 1, pp 670–675
35. Zordan V, Hodgins J (2002) Motion capture-driven simulations that hit and react. In: Proceedings of ACM SIGGRAPH/Europgraphics symposium on computer animation, pp 89–96
36. Witkin A, Kass M (1988) Spacetime constraints. In: SIGGRAPH '88: Proceedings of the 15th annual conference on computer graphics and interactive techniques. ACM, New York, NY, pp 159–168. doi:10.1145/54852.378507
37. Tak S, Ko HS (2005) A physically-based motion retargeting filter. ACM Trans Graph 24(1):98–117. doi:10.1145/1037957.1037963
38. Yamane K, Nakamura Y (2003) Dynamics filter-concept and implementation of online motion generator for human figures. In: Proceedings of the international conference on robotics and automation, vol 19, no. 3, pp 421–432
39. Muecke K, Hong D (2008) Investigation of an analytical motion filter for humanoid robots. In: Proceedings of the fifth international conference on ubiquitous robots and ambient intelligence
40. Muecke K (2009) An Analytical Motion Filter for Humanoid Robots. PhD Thesis, Virginia Polytechnic Institute and State University, Blacksburg, VA, USA
41. Hirai K (1998) The development of honda humanoid robot. In: Proceedings of the IEEE international conference on robotics and automation, pp 1321–1326

42. Ishida T (2003) A small biped entertainment robot sdr-4x ii. In: Proceedings of IEEE symposium on computational intelligence in robotics and automation, pp 1046–1051
43. Collins SH, Wisse M, Ruina A (2001) A three-dimensional passive-dynamic walking robot with two legs and knees. Int J Robotic Res 20(7):607–615
44. Vukobratovic M (2004) Zero-moment point–thirty five years of its life. Int J Humanoid Robotics 1(1):157–173
45. Vukobratovic M, Borovac B, Surla D, Stokic D (1990) Scientific fundamentals of robotics, vol 7: Biped locomotion. Springer, Berlin